

## Modeling streamflow and sediment responses to climate change and human activities in the Yanhe River, China

Jingwen Wu, Chiyuan Miao, Tiantian Yang, Qingyun Duan and Xiaoming Zhang

### ABSTRACT

Quantifying the impact of climate change and human activities on hydrological processes is of great importance for regional water-resource management. In this study, trend analysis and analysis of the short-term variations in annual streamflow and sediment load in the Yanhe River Basin (YRB) during the period 1972–2011 were conducted using linear regression and the Pettitt test. The Soil and Water Assessment Tool (SWAT) was employed to simulate the hydrological processes. The results show that both annual mean streamflow and annual mean sediment load in the YRB significantly decreased ( $P < 0.05$ ) during the study period. The relative contributions from climate change and human activities to YRB streamflow decline between 1996 and 2011 were estimated to be 55.8 and 44.2%, respectively. In contrast to the results for streamflow, the dominant cause of YRB sediment-load decline was human activity (which explained 64% of the decrease), rather than climate change. The study also demonstrates that topographical characteristics (watershed subdivision threshold value, digital elevation model spatial resolution) can cause uncertainties in the simulated streamflow and sediment load. The results presented in this paper will increase understanding of the mechanisms of soil loss and will enable more efficient management of water resources in the YRB.

**Key words** | climate change, human activities, sediment load, streamflow, SWAT, Yanhe River

**Jingwen Wu**

**Chiyuan Miao** (corresponding author)

**Qingyun Duan**

State Key Laboratory of Earth Surface Processes and Resource Ecology, College of Global Change and Earth System Science, Beijing Normal University, Beijing 100875, China

and

Joint Center for Global Change Studies, Beijing 100875, China

E-mail: [miaocy@vip.sina.com](mailto:miaocy@vip.sina.com)

**Tiantian Yang**

Department of Civil and Environmental Engineering, University of California, Irvine, CA 92697, USA

**Xiaoming Zhang**

State Key Laboratory of Simulation and Regulation of Water Cycle in River Basin, China Institute of Water Resources and Hydropower Research, Beijing 100048, China

### INTRODUCTION

Changes in the regional water cycle are closely related to water scarcity, which is a pressing issue across the world (Yan *et al.* 2016). Climate change and human activity are widely acknowledged to be key drivers of change in hydrological processes (Lin *et al.* 2007; Piao *et al.* 2007; Miao *et al.* 2010). Annual global land precipitation increased at a rate of  $\sim 0.2$  mm/yr during the 20th century (Piao *et al.* 2007) and global surface temperature has increased by  $\sim 0.8$  °C over the past century (Hansen *et al.* 2006). Global warming accelerates regional water cycles and transforms the intensity and frequency of precipitation, further affecting hydrological processes (IPCC 2007). Human activities, such as reservoir construction (Kong *et al.* 2015), soil and water conservation

(Ma *et al.* 2010), water abstraction (Weiskel *et al.* 2007), and alteration of land use due to urbanization and economic development (Schilling *et al.* 2010), cause great changes in natural river systems and hydrological cycles. Hydrological changes result directly in variations in streamflow and sediment load, which in turn can increase the frequency of flash flooding and the potential risks to the local ecosystem and environment. Quantifying the influence of climate change and human activities on hydrological processes is of value to policymakers and government agencies responsible for efficient water-resource and ecosystem management.

The Loess Plateau is the largest loess region in the world (Vasiljevic *et al.* 2014). It forms a substantial part

of the arid and semi-arid landscape, and the heterogeneity of the land surface is remarkable (Huang *et al.* 2008). Owing to the particular geographic landscape, centuries of excessive cultivation, and rapid population growth, the Loess Plateau has become one of the most seriously eroded areas in the world and its ecological environment is consequently fragile (Liu *et al.* 2011). The annual mean soil loss on the Loess Plateau is about 2,000–2,500 t/km<sup>2</sup> (Shi & Shao 2000) and the amount of earth and sand flowing out from the Loess Plateau to the Yellow River can reach 1.6 billion t/yr (Sun *et al.* 2015). The Yanhe River Basin (YRB) located in the center of the Loess Plateau, is a typical loess hilly–gully region, and has an average annual soil loss of 14,460 t/km<sup>2</sup>, causing enormous sedimentation in the Yellow River system and increased risk of flooding in downstream areas. Thus, since the 1950s, a number of soil and water conservation projects have been implemented in this region by the Chinese central government. For example, in 1999, the ‘Grain for Green’ program was initiated to control the continually deteriorating ecological environment (Su *et al.* 2011) and has had a substantial impact on eco-hydrological conditions in the YRB (Xu 2003; Huang *et al.* 2008; Zhang *et al.* 2010). Furthermore, Li *et al.* (2012) used six general climate models to project changes in climate on the Loess Plateau over the 21st century, and predicted further amplification of variations in climate change. Similarly, Li *et al.* (2011b) used four climate models and the Water and Erosion Prediction Project model to project changes in climate and hydrology for the period 2010–2030, and predicted a –2.6 to 17.4% change in precipitation, a 0.6–2.6 °C rise in maximum temperature, a 0.6–1.7 °C rise in minimum temperature, a 10–130% increase in runoff, and a –5 to 195% increase in soil loss. The YRB is a representative district within the Loess Plateau region, so future changes in climate in the YRB are likely to be similar to those predicted for the Loess Plateau as a whole. In order to provide better management of the water resources in the YRB under these anticipated changes in climate, it will be useful to distinguish the relative contributions of human activities and climate change on changes in streamflow and sediment load in this region.

Studies evaluating the impact of climate change and human activities on streamflow and sediment load have

proliferated in recent years (Miao *et al.* 2011; Zhang *et al.* 2014; Hao *et al.* 2015; Singh *et al.* 2015; Marhaento *et al.* 2017). Zhang *et al.* (2010) used a modified double-mass curve to show that reforestation and farmland terracing on the Loess Plateau reduced surface runoff by 20–100% and sediment yield by 10–100%. Zhu *et al.* (2015) employed two quantitative evaluation methods to separate the impact of climate change and anthropogenic activities on runoff changes: the result revealed climate change had an important role in runoff decline, accounting for about 60% of the change. Miao *et al.* (2011) utilized simple linear regression to evaluate the effects of climate change and human activities on changes in streamflow and sediment load, and showed that streamflow and sediment load in the upper reach of the Yellow River have decreased by 86 and 83%, respectively, over the past fifty years as a result of human activities.

There are two main categories of methods for distinguishing the effects of climate change and human activities on streamflow and sediment load: modeling methods and non-modeling methods. Compared with non-modeling methods, which lack representation of the potential physical mechanisms, modeling methods include complicated physical mechanisms, and can evaluate the effects of climate change and human activities on streamflow and sediment load over different time scales. Therefore, modeling methods have been widely used to assess the relative effects of climate change and human activities on hydrology (Li *et al.* 2009; Zhan *et al.* 2013). Therefore, in this study, we used the Soil and Water Assessment Tool (SWAT) to accurately distinguish the contributions of climate change and human activities on changes in streamflow and sediment load. We also discuss the effects of the digital-elevation-model (DEM) data resolution and watershed delineation on the SWAT-model prediction uncertainty.

The goals of this study are: (1) to evaluate the applicability of SWAT in simulating streamflow and sediment load in the YRB; (2) to jointly quantify the impact of climate change and human activity on variations in streamflow and sediment load in the YRB; (3) to analyze model uncertainty (e.g. watershed subdivision and DEM resolution). Through this study, we aim to improve understanding of the relationship between natural processes and human activities.

Furthermore, the simulation results will provide a valuable reference for government agencies and should enable more efficient management of water and soil in the YRB.

## MATERIALS AND METHODS

### Study area

The YRB, a tributary to the middle reaches of the Yellow River, is located in the central hilly region of the Loess Plateau in China, with longitude  $36^{\circ}21'N$ – $37^{\circ}19'N$  and latitude  $108^{\circ}38'E$ – $110^{\circ}29'E$  (Figure 1). The basin covers an area of  $7,485 \text{ km}^2$  at elevations ranging from 500 to 1,780 m (average elevation = 1,218 m) and has a typical warm temperate continental monsoonal climate. The annual mean temperature is  $9^{\circ}\text{C}$  and the annual mean precipitation is 495 mm. Over 65% of the annual precipitation falls in the summer monsoon period between June and September (Wang et al. 2010). The multi-year mean delivery modules for streamflow and sediment load in the YRB are  $3.64 \times 10^4 \text{ m}^3/\text{km}^2 \text{ yr}$  and  $7.8 \times 10^4 \text{ t}/\text{km}^2 \text{ yr}$ , respectively (Su et al. 2012). Soil erosion induced by long-term incision has resulted in approximately 90% of the YRB being covered with ridges and gullies (Fu et al. 2005).

Land use in this area includes cultivation, grassland, forest, water, urban areas, and bare land.

### Data source

SWAT requires topographical, land-use, soil, and meteorological information. Topographical data were derived from a DEM with a resolution of  $20 \times 20 \text{ m}$ , obtained from the Resources and Environmental Science Data Center, Chinese Academy of Sciences ([www.resdc.cn/](http://www.resdc.cn/)). Land-use data for the years 1990 and 2010 were also obtained from the Resources and Environmental Science Data Center, Chinese Academy of Sciences ([www.resdc.cn/](http://www.resdc.cn/)). Land-use data for the year 1980 were obtained from the Soil Survey Office for Shanxi Province, and was used in the calibration and validation periods. Soil data, including a soil type map (1:1,000,000) and soil properties, were retrieved from the Cold and Arid Regions Science Data Center, Chinese Academy of Sciences ([westdc.westgis.ac.cn/](http://westdc.westgis.ac.cn/)). Daily meteorological data from 11 weather stations were obtained from the China Meteorological Data Sharing Service System ([www.escience.gov.cn/](http://www.escience.gov.cn/)). Ganguyi station is located at the outlet of the YRB watershed. It controls 77% of the entire drainage basin and was the

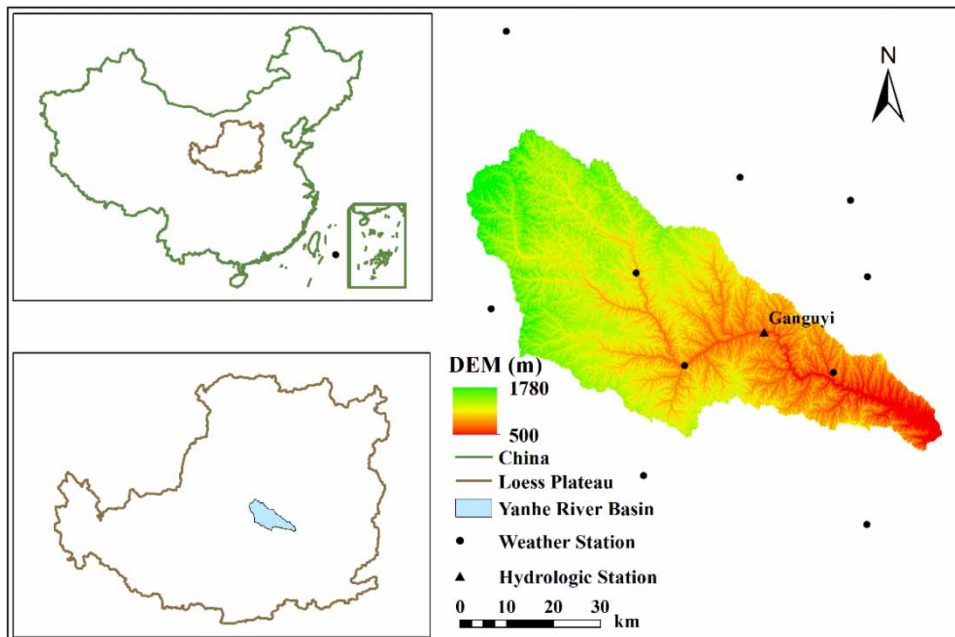


Figure 1 | Location of YRB and its hydrological and weather stations.

only station in this study. Monthly streamflow and sediment load data from Ganguyi station from 1972 to 2011 were obtained from the Yellow River Commission Committee, and were used for model calibration and validation.

### Abrupt change analysis

The Pettitt test (Pettitt 1979) is widely used in hydro-climatological studies to detect abrupt changes in the mean of variables of interest. The change point detected by the Pettitt test reflects the most significant change in the variable mean between two periods. The two samples  $(x_1 \dots x_z)$  and  $(x_{z+1} \dots x_{zn})$  come from the same population. The statistical index  $U_{zn}$  is given by:

$$U_{zn} = \sum_{i=1}^z \sum_{j=i+1}^n \text{sgn}(x_i - x_j) \quad \text{if } z = 2, \dots, n \quad (1)$$

$$\text{sgn}(x) = \begin{cases} 1 & x > 0 \\ 0 & x = 0 \\ -1 & x < 0 \end{cases} \quad (2)$$

The abrupt change point is defined as the point where  $U_{zn}$  reaches its maximum value, and the associated probability ( $P$ ) is given as:

$$k_n = \max|U_{zn}| \quad (3)$$

$$P = \exp \left[ \frac{-6(k_n)^2}{(n^3 + n^2)} \right] \quad (4)$$

If  $P$  is smaller than the specified significance level, which is 0.05 in this study, the null hypothesis is rejected.

### SWAT model and sensitivity analysis

SWAT, developed by the United States Department of Agriculture, is a semi-distributed hydrological model (Arnold et al. 2012). The SWAT model is able to predict the long-term impacts of land use and agricultural management on water under varying soil, land-use, and management conditions (Arnold et al. 1998). The main components of the SWAT model are climate, hydrology, land cover and plant growth, erosion, nutrients, pesticides, management, and channel routing. In the SWAT

model, surface runoff is estimated with the Soil Conservation Service (SCS) runoff curve number (CN) method (SCS 1972) and sediment yield is calculated from the Modified Universal Soil Loss Equation (MUSLE) developed by Williams & Berndt (1977). More detailed information about the SWAT model can be found in Arnold et al. (1998).

In this study, the 10 most sensitive parameters for the streamflow and sediment load simulations identified by SWAT Calibration and Uncertainty Procedures are listed in Tables S1 and S2 (supplementary material, available with the online version of this paper), together with their detailed definitions, ranges, optimum values, and sensitivity ranks. The SCS runoff curve number II(CN2) was the most sensitive parameter for both streamflow and sediment load simulations.

### Model set up and calibration

The ArcSWAT 2012 (Rev.627) interface was used to set up and parameterize the model. From examination of the 20 m DEM data and the stream network, a threshold drainage area of 100 km<sup>2</sup> was chosen to delineate the watershed, and the watershed was divided into 46 sub-basins. We further sub-divided the sub-basins into 134 different hydrological response units (HRUs) on the basis of land use, soil, and slope class thresholds of 10, 15, and 10%, respectively. We then set up the SWAT model using meteorological data from 1972 to 2011: 1970–1971 was used for the warm-up period, 1972–1978 was used for the calibration period, 1979–1982 was used for the validation period. Streamflow and sediment load were calibrated and validated separately, and the impact of climate change and human activities on changes in streamflow and sediment load were also assessed separately. The performance of the simulated results was evaluated by the Nash–Sutcliffe model efficiency ( $NSE$ ) (Nash & Sutcliffe 1970) and by the correlation coefficient ( $R$ ). The calculations for these two measures are:

$$NSE = 1 - \frac{\sum (Q_o - Q_m)^2}{\sum (Q_o - \bar{Q}_o)^2} \quad (5)$$

$$R = \frac{\sum (Q_o - \bar{Q}_o)(Q_m - \bar{Q}_m)}{\sqrt{\sum (Q_m - \bar{Q}_m)^2 \sum (Q_o - \bar{Q}_o)^2}} \quad (6)$$

where  $Q_o$  and  $Q_m$  are the observations and the simulation, respectively, and  $\overline{Q_o}$  and  $\overline{Q_m}$  are the means of the corresponding variables.  $NSE$  ranges from  $-\infty$  to 1, and  $R$  ranges from  $-1$  to 1. The closer the values of  $NSE$  and  $R$  are to 1, the more similar the simulation is to the observations.

### Quantification of the impacts of climate change and human activity on streamflow and sediment load

Streamflow and sediment load are simultaneously affected by climate variability and human interference. On the basis of the results of the abrupt change analysis, the time-series for streamflow and sediment load were divided into two sub-periods, termed the baseline or ‘pre-change’ period and the evaluation or ‘post-change’ period. For a given watershed, we assumed that the total change in annual mean flow or sediment load can be calculated as:

$$\Delta Q_t = Q_v - Q_b \quad (7)$$

where  $\Delta Q_t$  indicates the total change and  $Q_v$  and  $Q_b$  are the observations during the evaluation period and the baseline period. Assuming the total change  $\Delta Q_t$  comes from the combined effects of climate change and human activities, the following decomposition can be carried out:

$$\Delta Q_t = \Delta Q_c + \Delta Q_h \quad (8)$$

$$\Delta Q_c = Q_{vs} - Q_{bs} \quad (9)$$

where  $\Delta Q_c$  indicates the hydrological changes caused by climate change and  $\Delta Q_h$  indicates the changes caused by

human activity. First, the model is calibrated and validated for the time period furthest in the past, then the model is run during the evaluation period without considering any human impacts. The difference in modeled streamflow before and after the change point can therefore be attributed to climate change only, and ‘unexplained’ changes not depicted by the model are then attributed to the effect of human influence.  $Q_{vs}$  and  $Q_{bs}$  are the simulated results using climate data in the evaluation and baseline periods, respectively. Therefore, the percentage contributions from climatic change ( $P_c$ ) and human activity ( $P_h$ ) on the variations in streamflow and sediment load can be described as:

$$P_c = \frac{\Delta Q_c}{\Delta Q_t} \times 100\% \quad (10)$$

$$P_h = \frac{\Delta Q_h}{\Delta Q_t} \times 100\% \quad (11)$$

## RESULTS

### Statistical analysis of streamflow and sediment load data

Figure 2 shows the variations in observed annual streamflow and sediment load in the YRB between 1972 and 2011. As shown in Figure 2, streamflow and sediment load both had significant downward trends ( $P < 0.05$ ) over that time period. The yields decreased at approximately  $0.77 \text{ m}^3/\text{s}$  per year (annual streamflow) and  $0.76 \times 10^6 \text{ t}$  per year (annual sediment load). The variations in streamflow and sediment

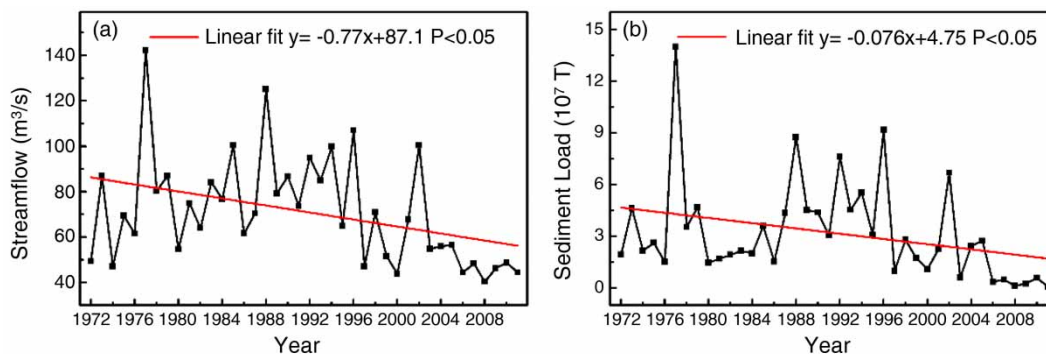


Figure 2 | Variations in annual streamflow (a) and sediment load (b) between 1972 and 2011 in the YRB.



load were similar to each other during the period 1972–2011, with the highest values occurring in 1978 and the lowest values occurring in 2008.

Figure 3 shows the changes in the annual streamflow and sediment load time-series, as detected with the Pettitt test. Both streamflow and sediment load series were subject to an abrupt change in 1996. We therefore further divided the series into two sub-periods: the baseline period (before 1996) and the evaluation period (after 1996). We found that annual mean streamflow was  $81.1 \text{ m}^3/\text{s}$  before 1996 and  $54.8 \text{ m}^3/\text{s}$  after 1996. Similarly, the annual mean sediment load was  $4.2 \times 10^7 \text{ t}$  before 1996 and  $1.5 \times 10^7 \text{ t}$  after 1996. Annual mean streamflow and annual mean sediment load dropped by 32.4 and 63.0% in the evaluation period compared with the baseline period.

### Evaluation of streamflow and sediment load simulations

Figure 4 shows the simulated YRB streamflow and sediment load during the calibration (1972–1978) and validation (1979–1982) periods. In general, the magnitude and variation of the simulations were similar to the observations. The statistical measurements are presented in Table S3 in the supplementary material (available with the online version of this paper). For streamflow,  $R^2$  and  $NSE$  were 0.81 and 0.71 in the calibration period and 0.74 and 0.65 in the validation period. SWAT performance was not as good for the sediment load simulation as for the streamflow simulation:  $R^2$  and  $NSE$  were 0.71 and 0.73 in the calibration period and 0.64 and 0.81 in the validation period.

As shown in Figure 4, the general magnitude and variation of the simulated streamflow and sediment load were

similar to the observations. Both streamflow and sediment load simulations achieved high  $R^2$  and  $NSE$  values in the calibration and validation periods (Table S3). However, most of the disagreements between the model and observations occurred at the peak values. For example, during the highest peak (around August 1977) the model overestimated streamflow and underestimated sediment load. The nonlinear relationships between meteorological elements and streamflow (or sediment load) make the simulation complex, especially for extreme events. In addition, we could not take check dams into consideration owing to the unacceptability of the data; however, surface streamflow and sediment yield in the rainy season and annually will be reduced because of interception by check dams (Xu et al. 2013). Furthermore, daily hydrologic data are not available and the monthly data do not reflect individual events well.

### Impacts of climate change and human activities on streamflow and sediment load

Table 1 shows the calculated contributions from climate change and human activities to the total streamflow and sediment load reduction in the YRB during the period 1996–2011. As shown in Table 1, the climate-change-induced streamflow decrease was  $14.7 \text{ m}^3/\text{s}$  per year, which accounts for 55.8% of the total decrease. The remaining 44.2% of streamflow reduction was attributed to human activities. For sediment load, climate change and human activities contributed about 36 and 64% of the total sediment load decrease, respectively. Thus, during the evaluation period (1996–2011) climate change had a larger impact on streamflow decline than human activities,

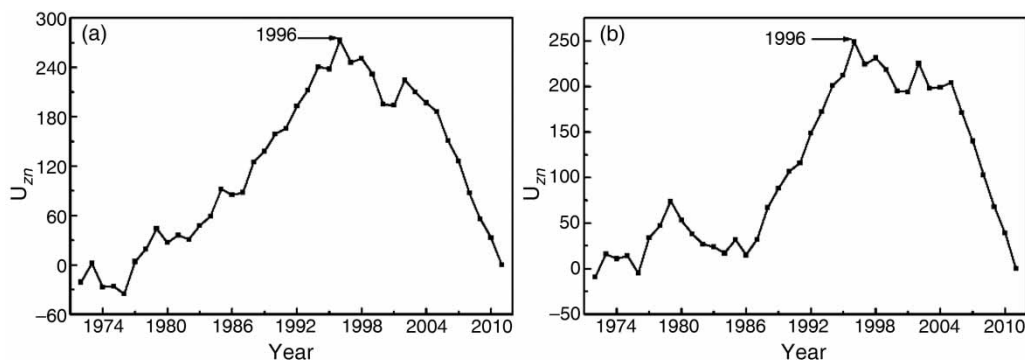
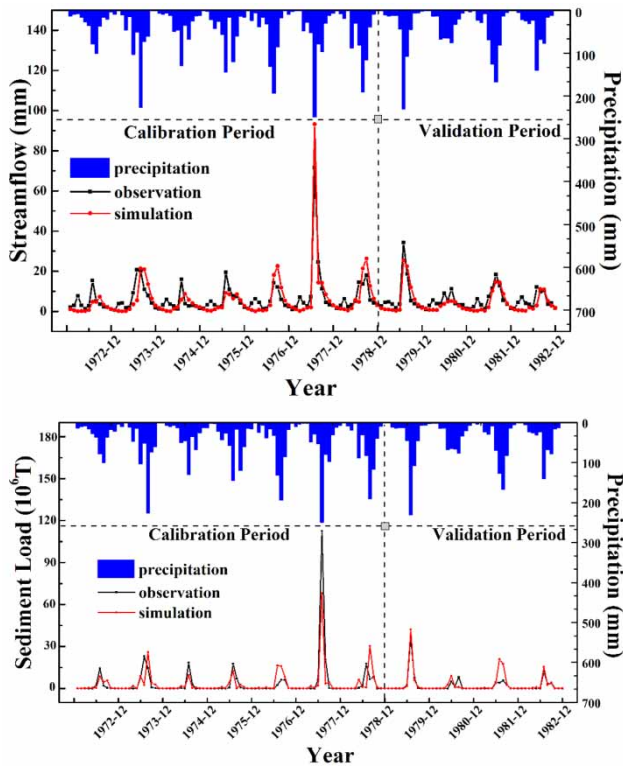


Figure 3 | The abrupt change in streamflow (a) and sediment load (b), as detected by the Pettitt test.



**Figure 4** | Observed and simulated monthly streamflow (top) and sediment load (bottom) in the YRB during the calibration period (1972–1978) and the validation period (1979–1982).

whereas human activities were the main cause of the decline in sediment load.

## DISCUSSION

### Impact of climate change and human activities

Climate change and human activity are the major drivers of changes in streamflow and sediment load at the

watershed scale. Generally speaking, temperature and precipitation are the dominant climate factors that impact the streamflow and sediment load yields (Morin *et al.* 2006; Wei *et al.* 2007; Nadal-Romero *et al.* 2008; Miao *et al.* 2015). Rising temperatures can significantly increase evaporation and extend the growing season, and decreasing precipitation directly reduces streamflow. Figure 5 displays the variations in annual mean temperature and precipitation for the YRB between 1972 and 2011. Annual mean temperature showed a significant upward trend over that time period ( $P < 0.01$ ), with an estimated increase of  $0.04\text{ }^{\circ}\text{C}$  per year. Annual mean precipitation showed a downward trend, with an estimated decrease of  $0.05\text{ mm/yr}$ . Further examination reveals that precipitation in the wet season (May–September) during the evaluation period was lower than wet-season precipitation during the baseline period. Daily precipitation over 10 and 20 mm thresholds occurred much more frequently during the baseline period than during the evaluation period. Most of the rain falls during the wet season and is associated with high-intensity precipitation events. The decreases in streamflow and sediment load during the evaluation period were likely partly due to these changes in temperature and precipitation patterns.

Assessing the individual impacts of human activities on streamflow and sediment load is relatively complex because there are many human factors that can influence the streamflow and sediment load both directly and indirectly. The water demand from different sectors for the YRB is listed in Table 2. With the development of the urban economy and the increasing urban population, it is inevitable that the demand for water will gradually expand. Domestic, agricultural, and industrial water use increased by 224, 111, and 156%, respectively between

**Table 1** | Estimated contributions from climate change and human activities to streamflow and sediment load in the YRB

|                                      | Period     | $Q_o$             | $Q_s$             | $\Delta Q_t$       | Climate change (%) | Human activity (%) |
|--------------------------------------|------------|-------------------|-------------------|--------------------|--------------------|--------------------|
| Streamflow ( $\text{m}^3/\text{s}$ ) | Baseline   | 81.1              | 59.6              |                    |                    |                    |
|                                      | Evaluation | 54.8              | 44.9              | -26.3              | 55.8               | 44.2               |
| Sediment load (ton)                  | Baseline   | $4.2 \times 10^7$ | $3.6 \times 10^7$ |                    |                    |                    |
|                                      | Evaluation | $1.5 \times 10^7$ | $2.7 \times 10^7$ | $-2.6 \times 10^7$ | 36                 | 64                 |

$Q_o$  denotes the observed streamflow and sediment load data in both periods.  $Q_s$  denotes the simulated streamflow and sediment load values in both periods.  $\Delta Q_t$  denotes the total changes during these two period (observed data in the evaluation period minus observed data in the baseline period).

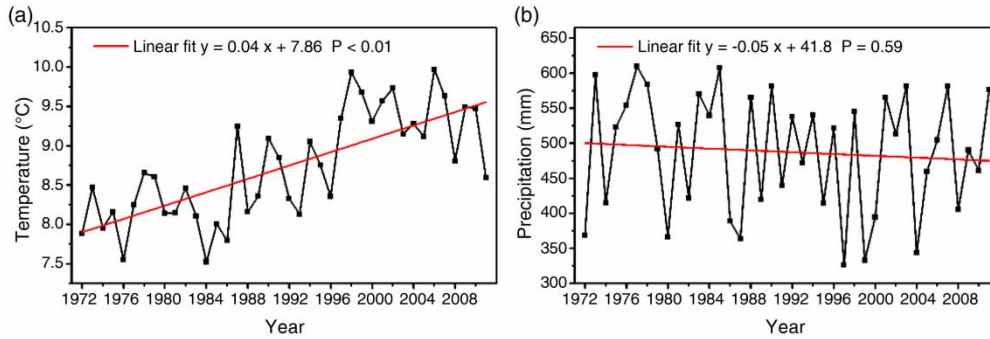


**Figure 5** | Annual mean temperature (a) and precipitation (b) in the YRB from 1972 to 2011.

**Table 2** | Water consumption in the YRB

| Consumption type   | Water consumption ( $10^4 \text{ m}^3$ ) |          |          |          |          |
|--------------------|--|----------|----------|----------|----------|
|                    | 1980                                     | 1985     | 1990     | 1995     | 2000     |
| Domestic water     | 531.1                                    | 590.83   | 710.28   | 898.48   | 1,188.13 |
| Agricultural water | 884.37                                   | 915.81   | 939.39   | 959.04   | 978.71   |
| Industrial water   | 1,123.38                                 | 1,269.45 | 1,415.52 | 1,561.59 | 1,756.35 |

Data obtained from Wang et al. (2010).

1980 and 2000. Hence, the direct influence of human activities on streamflow has intensified over the years.

However, the influence of human activities on streamflow and sediment load is mainly indirect. Human activities change the natural geographical conditions of a basin through changing land use and soil and water conservation projects, which in turn alter the hydrological processes. There have been many previous reports showing that land-use changes are associated with changes in the hydrological

processes (Li et al. 2009; Zhang et al. 2010). Figure 6 shows the area covered by different land-use categories in the YRB in 1990 and 2010, and Table S4 (supplementary material, available with the online version of this paper) displays the corresponding statistics. Between 1990 and 2010, the total area covered by grassland decreased by  $44.67 \text{ km}^2$  and the total area covered by water decreased by  $5.59 \text{ km}^2$ . Urban areas increased by  $8.94 \text{ km}^2$  and areas of bare land increased by  $0.13 \text{ km}^2$ . There was also an increase of  $250.27 \text{ km}^2$  in

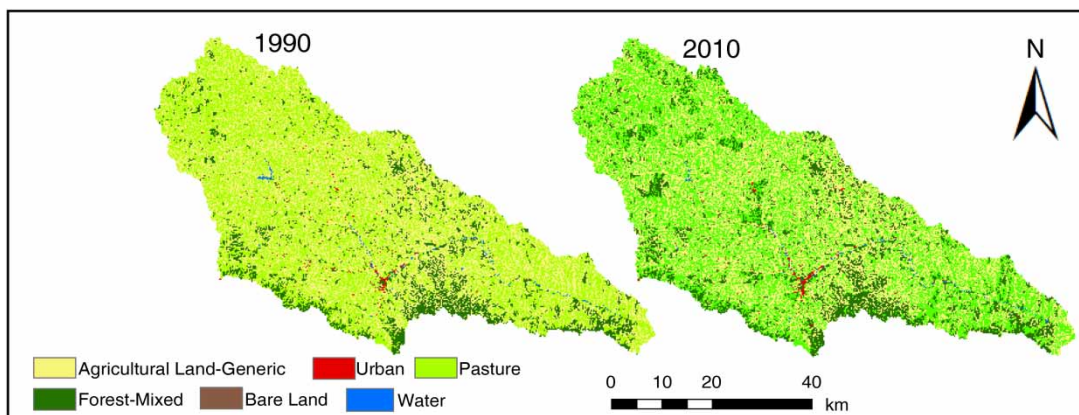


**Figure 6** | Land use in 1990 and 2010 in the YRB.



forestland and a decrease of about 200 km<sup>2</sup> in cropland. This change was primarily caused by the intentional conversion of land from crops to forest and grass, which is the focus of the ‘Grain for Green’ program (Su *et al.* 2012). However, even after adjusting for the effects of the ‘Grain for Green’ program, the area of land given over to all types of soil and water conservation measures has increased since 2000. More intensive vegetation decreases streamflow via the interception of rainfall by the vegetation canopy. Meanwhile, increases in vegetation may also increase the infiltration and evapotranspiration rates, leading to further reductions in streamflow and sediment load.

The YRB is one of the areas on the Loess Plateau that suffers from severe soil erosion. To control soil erosion, many soil and water conservation measures have been implemented in the YRB, including terracing, check-dam construction, forestation, and grass planting. Table 3 shows the cumulative land area in the YRB given over to major soil and water conservation measures during different time periods. As shown in Table 3, the cumulative conservation area increased dramatically after the 1980s. Such large-scale implementation of soil and water conservation measures can change the characteristics of soil structures under the surface (micro-topography, land cover, and soil features), as well as altering the local energy and water balance (Yang *et al.* 2009). For example, a check dam can reduce streamflow and sediment load directly by retaining floodwater and intercepting soil sediment, and can also reduce them indirectly by increasing the evaporation and soil water storage (Xu *et al.* 2013). Terracing decreases the slope of the hillside, promoting the infiltration in the soil

profile weakening soil erosion, and thus reducing streamflow and sediment load. Therefore, the increasingly intensive soil and water conservation practices may play an important role in reducing streamflow and sediment load in the YRB.

In this study, the results indicate that the impact of climate change exceeds that of human activities to reductions in streamflow, and accounts for 55.8% of the total decrease. Previous studies on this topic in the YRB have not yet reached a consistent conclusion. Gao *et al.* (2015) demonstrated using the Budyko equation that climatic variability contributed 49% of the change in streamflow. Different methods and different research periods may therefore lead to different results. However, most studies have shown that human activities play a significant role in the change in sediment load in the YRB – about 65–85% of the total decline in most studies (Qiu 2012; Cheng *et al.* 2016). Soil and water conservation measures, such as check dams, may influence sediment load more significantly than streamflow. Therefore, on the one hand, we should improve the model simulations in order to predict streamflow and sediment load more accurately in the future and, on the other hand, we should continue to carry out soil and water conservation measures in the YRB.

### Impact of watershed subdivision threshold value and DEM resolution

In SWAT, the different watershed subdivision thresholds (WST) and DEM spatial resolutions can affect the watershed modeling process and subsequent results (Jha *et al.*

**Table 3** | Cumulative area used for major soil and water conservation practices in the YRB

| Conservation measures        | Incremental area of conservation measures (km <sup>2</sup> ) |                |                  |                 |                 |
|------------------------------|--|----------------|------------------|-----------------|-----------------|
|                              | 1970–1979  | 1980–1989      | 1990–1996        | 1997–2000       | 2001–2005       |
| Terracing                    | 50.33  | 76.8           | 101.27           | –56             | 65.9            |
| Check dams                   | 12.9   | 9.07           | 3.87             | –4.57           | 12.4            |
| Forestation                  | 125.66   | 553.8          | 259.47           | 557.3           | 491.3           |
| Grass planting               | 13.74  | 127.73         | 114.67           | –79.47          | 54.1            |
| Total conservation area      | 202.63   | 767.4          | 479.28           | 900.06          | 783.2           |
| Cumulative conservation area | 430.66 (5.7%)  | 1,198.06 (16%) | 1,677.34 (22.4%) | 2,577.4 (34.4%) | 3,350.6 (44.8%) |

Data obtained from Li *et al.* (2011a).

2004; Chaubey et al. 2005). The WST reflects the minimum drainage area required to form the origin of a stream. Once the WST is assigned a subjective value, SWAT automatically delineates the sub-watersheds, and further subdivides these sub-watersheds into HRUs. The DEM data contain the topography of the study area, which plays an important role in the hydrological cycle. Thus, in order to evaluate the sensitivity of the simulation to the WST and DEM resolution, 10 different WST levels ranging from 20 to 500 km<sup>2</sup> and 11 DEM spatial resolutions ranging from 20×20 to 2,000×2,000 m were used to simulate annual streamflow and sediment load during the period 1972–1978, and then the uncertainties were compared.

The simulated annual streamflow and sediment load under different WST levels are shown in Figure S1 (supplementary material, available with the online version of this paper). We found that changing the WST barely changed the simulated streamflow, consistent with the results from previous studies (FitzHugh & Mackay 2000; Jha et al. 2004; Tripathi et al. 2005). Surprisingly, in the sediment-load experiment, changing the WST tended to dramatically influence the sediment load during the years with large sediment yields. In other words, the WST can bring a considerable degree of uncertainty to the sediment load simulation. In SWAT, the sediment yield is calculated by the MUSLE, as follows:

$$\text{Sediment Yield} = 11.8(Q_{\text{surf}} \cdot q_{\text{peak}} \cdot \text{Area})^{0.56} \cdot K \cdot C \cdot P \cdot LS \cdot CFRG \quad (12)$$

where  $Q_{\text{surf}}$  is the daily runoff volume;  $q_{\text{peak}}$  is the 30-minute peak runoff rate; Area is the HRU area; and  $K$ ,  $C$ ,  $P$ ,  $LS$ , and

$CFRG$  are the soil erodibility, cover and management, support practice, topographic, and coarse fragment factors, respectively. As shown in Equation (12), a smaller WST value will lead to a larger number of sub-watersheds and a reduction in the mean sub-watershed area (Table S5 in the supplementary material, available with the online version of this paper). However,  $q_{\text{peak}}$  changes in proportion to the HRU area (Neitsch et al. 2004): when the WST is low, the value of  $q_{\text{peak}}$  will also be low and, consequently, the sediment yield will be reduced (Equation (12)). Furthermore, there is a nonlinear dependency of sediment yield on 'Area' because area is raised to the power of 0.56. In addition, if the WST value exceeds a certain threshold (150 km<sup>2</sup> in this research), the stream length and stream slope for the watersheds at the watershed outlet (WOS) will show a large change (Table S5), thus influencing sediment load during the years with large yield.

Simulated streamflow and sediment load tend to decrease with coarser spatial resolution (Figure S2 in supplementary material, available with the online version of this paper). Moreover, we found that there is a DEM resolution threshold beyond which the simulation results become extremely unstable. As shown in Figure S2, a robust estimate of this DEM threshold for the YRB is approximately 100×100 m. Delineation of sub-watersheds is reliant on topographical accuracy, and topographical features are lost when the DEM resolution reaches a certain level of coarseness. As the DEM resolution becomes coarser, the mean slope is reduced and the total watershed tends to be flatter (Table S6 in the supplementary material, available with the online version of this paper). Streamflow

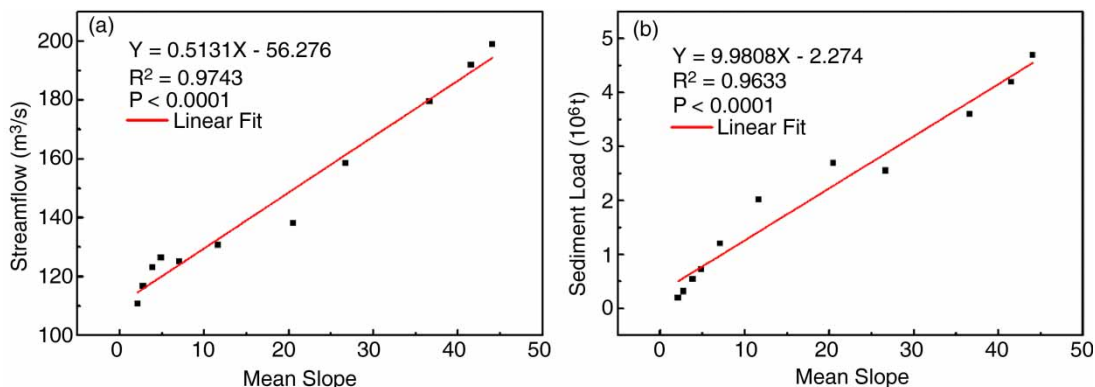


Figure 7 | Correlation between the mean slope and (a) streamflow and (b) sediment load.

and sediment load in SWAT are significantly correlated with the mean slope, with  $R^2$  of 0.97 and 0.96 for streamflow and sediment load, respectively (Figure 7). Some previous studies have shown that DEM resolution has no effect on SWAT simulated streamflow, but those results were likely due to the research area being flat (e.g. Chaplot 2005) or small with dense cover (e.g. Lin *et al.* 2013). In our opinion, the relationship between DEM resolution and simulated streamflow likely varies according to the region being studied.

## CONCLUSIONS

Climate change and human activity are key factors that significantly affect streamflow and sediment-load patterns at the watershed-scale. In this paper, we aimed to quantify the impact of climate variability and human activities on changes in streamflow and sediment load in the YRB. In addition, we also specifically assessed the sensitivity of the streamflow and sediment-load simulations to different SWAT model configurations (WST value and DEM resolution). Our major findings are summarized as follows:

The annual mean temperature in the YRB showed a significant upward trend during the period 1972–2011, but no significant trend was observed for annual mean precipitation. Both annual mean streamflow and annual mean sediment load in the YRB decreased significantly ( $P < 0.05$ ) during that time period. The SWAT model performed well in simulating the YRB streamflow and sediment load.

The WST level had almost no effect on the streamflow simulation. However, for years in which there was a large sediment load, the simulated sediment yield increased significantly above the observed values as the selected WST value increased, for WST values above a certain threshold (150 km<sup>2</sup> in this research). Both streamflow and sediment load tended to have smaller simulated values when the DEM resolution was decreased.

Climate change played a slightly larger role in changes in YRB streamflow during the period 1996–2011, contributing 55.8% of the total decrease in streamflow. In contrast, human activities were responsible for approximately 64% of the total decrease in sediment load during the same period. Therefore, human activities appear to have a greater effect

than climate change on sediment load. The results presented in this paper should enable a better understanding of the intrinsic causes of change in the hydrological cycle and sediment transport processes on the Loess Plateau. In addition, the findings on streamflow variability and sediment-load changes in the YRB could be a useful reference for adjusting current water-resource management plans and evaluating the potential risks to the ecosystem and environment.

## ACKNOWLEDGEMENTS

This research was supported by the National Natural Science Foundation of China (No. 41622101), the National Key Research and Development Program of China (No. 2016YFC0501604; No. 2016YFC0402407), and the State Key Laboratory of Earth Surface Processes and Resource Ecology. We are grateful to the Yellow River Conservancy Commission of the Ministry of Water Resources ([www.yellowriver.gov.cn/](http://www.yellowriver.gov.cn/)) for collecting and archiving the dataset of population and water conservancy facilities in the Yellow River Basin, and to the organization of the Yellow River ([www.yellowriver.org/](http://www.yellowriver.org/)) for collecting and archiving the soil and water conservation data in the Yellow River Basin.

## REFERENCES

- Arnold, J. G., Srinivasan, R., Muttiah, R. S. & Williams, J. R. 1998 Large area hydrologic modeling and assessment – Part 1: model development. *J. Am. Water Resour. Assoc.* **34**, 73–89.
- Arnold, J. G., Moriasi, D. N., Gassman, P. W., Abbaspour, K. C., White, M. J., Srinivasan, R., Santhi, C., Harmel, R. D., van Griensven, A., Van Liew, M. W., Kannan, N. & Jha, M. K. 2012 SWAT: model use, calibration, and validation. *Trans. ASABE* **55**, 1491–1508.
- Chaplot, V. 2005 Impact of DEM mesh size and soil map scale on SWAT runoff, sediment, and NO<sub>3</sub>-N loads predictions. *J. Hydrol.* **312**, 207–222.
- Chaubey, I., Cotter, A. S., Costello, T. A. & Soerens, T. S. 2005 Effect of DEM data resolution on SWAT output uncertainty. *Hydrol. Process.* **19**, 621–628.
- Cheng, Y., He, H., Cheng, N. & He, W. 2016 The effects of climate and anthropogenic activity on hydrologic features in Yanhe River. *Adv. Meteorol.* **2016**, 1–11.
- FitzHugh, T. W. & Mackay, D. S. 2000 Impacts of input parameter spatial aggregation on an agricultural nonpoint source pollution model. *J. Hydrol.* **236**, 35–53.

- Fu, B. J., Zhao, W. W., Chen, L. D., Zhang, Q. J., Lu, Y. H., Gulinck, H. & Poesen, J. 2005 Assessment of soil erosion at large watershed scale using RUSLE and GIS: a case study in the Loess Plateau of China. *Land Degrad. Dev.* **16**, 73–85.
- Gao, P., Jiang, G. T., Wei, Y. P., Mu, X. M., Wang, F., Zhao, G. J. & Sun, W. Y. 2015 Streamflow regimes of the Yanhe River under climate and land use change, Loess Plateau, China. *Hydrol. Process.* **29**, 2402–2413.
- Hansen, J., Sato, M., Ruedy, R., Lo, K., Lea, D. W. & Medina-Elizade, M. 2006 Global temperature change. *Proc. Natl. Acad. Sci.* **103**, 14288–14293.
- Hao, Z. C., Chen, S. C., Li, Z. H., Yu, Z. B., Shao, Q. X., Yuan, F. & Shi, F. X. 2015 Quantitative assessment of the impacts of irrigation on surface water fluxes in the Tarim River, China. *Hydrol. Res.* **46** (6), 996–1007.
- Huang, J. P., Zhang, W., Zuo, J. Q., Bi, J. R., Shi, J. S., Wang, X., Chang, Z. L., Huang, Z. W., Yang, S., Zhang, B. D., Wang, G. Y., Feng, G. H., Yuan, J. Y., Zhang, L., Zuo, H. C., Wang, S. G., Fu, C. B. & Chou, J. F. 2008 An overview of the semi-arid climate and environment research observatory over the Loess Plateau. *Adv. Atmos. Sci.* **25**, 906–921.
- IPCC 2007 *Climate Change 2007: The Physical Science Basis*. Contribution of working group I to the fourth assessment report of the intergovernmental panel on climate change. Cambridge University Press, Cambridge, UK and New York, USA, pp. 10–18.
- Jha, M., Gassman, P. W., Secchi, S., Gu, R. & Arnold, J. 2004 Effect of watershed subdivision on swat flow, sediment, and nutrient predictions. *J. Am. Water Resour. Assoc.* **40**, 811–825.
- Kong, D. X., Miao, C. Y., Borthwick, A. G. L., Duan, Q. Y., Liu, H., Sun, Q. H., Ye, A. Z., Di, Z. H. & Gong, W. 2015 Evolution of the Yellow River Delta and its relationship with runoff and sediment load from 1983 to 2011. *J. Hydrol.* **520**, 157–167.
- Li, Z., Liu, W. Z., Zhang, X. C. & Zheng, F. L. 2009 Impacts of land use change and climate variability on hydrology in an agricultural catchment on the Loess Plateau of China. *J. Hydrol.* **377**, 35–42.
- Li, C. Z., Wang, H., Yu, F. L., Yang, A. M. & Yan, D. H. 2011a Impact of soil and water conservation on runoff and sediment in Yanhe River basin. *Sci. Soil Water Conserv.* **9** (1), 1–8.
- Li, Z., Liu, W. Z., Zhang, X. C. & Zheng, F. L. 2011b Assessing the site-specific impacts of climate change on hydrology, soil erosion and crop yields in the Loess Plateau of China. *Clim. Change* **105** (1–2), 223–242.
- Li, Z., Zheng, F. L., Liu, W. Z. & Jiang, D. J. 2012 Spatially downscaling GCMs outputs to project changes in extreme precipitation and temperature events on the Loess Plateau of China during the 21st Century. *Global Planet. Change* **82–83**, 65–73.
- Lin, Y. P., Hong, N. M., Wu, P. J. & Lin, C. J. 2007 Modeling and assessing land-use and hydrological processes to future land-use and climate change scenarios in watershed land-use planning. *Environ. Geol.* **53**, 623–634.
- Lin, S. P., Jing, C. W., Coles, N. A., Chaplot, V., Moore, N. J. & Wu, J. P. 2013 Evaluating DEM source and resolution uncertainties in the Soil and Water Assessment Tool. *Stoch. Environ. Res. Risk Assess.* **27**, 209–221.
- Liu, X. H., He, B. L., Li, Z. X., Zhang, J. L., Wang, L. & Wang, Z. 2011 Influence of land terracing on agricultural and ecological environment in the loess plateau regions of China. *Environ. Earth Sci.* **62** (4), 797–807.
- Ma, H. A., Yang, D. W., Tan, S. K., Gao, B. & Hu, Q. F. 2010 Impact of climate variability and human activity on streamflow decrease in the Miyun Reservoir catchment. *J. Hydrol.* **389** (3–4), 317–324.
- Marhaento, H., Booij, M. J. & Hoekstra, A. Y. 2017 Attribution of changes in stream flow to land use change and climate change in a mesoscale tropical catchment in Java, Indonesia. *Hydrol. Res.* **48** (4), 1143–1155. DOI:10.2166/nh.2016.110.
- Miao, C. Y., Ni, J. R. & Borthwick, A. G. L. 2010 Recent changes in water discharge and sediment load of the Yellow River basin, China. *Prog. Phys. Geog.* **34** (4), 541–561.
- Miao, C. Y., Ni, J. R., Borthwick, A. G. L. & Yang, L. 2011 A preliminary estimate of human and natural contributions to the changes in water discharge and sediment load in the Yellow River. *Global Planet. Change* **76**, 196–205.
- Miao, C. Y., Ashouri, H., Hsu, K., Sorooshian, S. & Duan, Q. Y. 2015 Evaluation of the PERSIANN-CDR daily rainfall estimates in capturing the behavior of extreme precipitation events over China. *J. Hydrometeorol.* **16**, 1387–1396.
- Morin, E., Goodrich, D. C., Maddox, R. A., Gao, X. G., Gupta, H. V. & Sorooshian, S. 2006 Spatial patterns in thunderstorm rainfall events and their coupling with watershed hydrological response. *Adv. Water Resour.* **29**, 843–860.
- Nadal-Romero, E., Regues, D. & Latron, J. 2008 Relationships among rainfall, runoff, and suspended sediment in a small catchment with badlands. *Catena* **74**, 127–136.
- Nash, J. E. & Sutcliffe, J. V. 1970 River flow forecasting through conceptual models part I – a discussion of principles. *J. Hydrol.* **10**, 9.
- Neitsch, S., Arnold, J., Srinivasan, R. & Williams, J. 2004 *Soil and Water Assessment Tool Input/Output File Documentation, Version 2005*. Blackland Research Center, USDA Agricultural Research Service, Temple, TX, pp. 1–431.
- Pettitt, A. N. 1979 A non-parametric approach to the change point problem. *J. R. Stat. Soc.* **28** (2), 126–135.
- Piao, S. L., Friedlingstein, P., Ciais, P., de Noblet-Ducoudre, N., Labat, D. & Zaehle, S. 2007 Changes in climate and land use have a larger direct impact than rising CO<sub>2</sub> on global river runoff trends. *Proc. Natl. Acad. Sci.* **104**, 15242–15247.
- Qiu, L. J. 2012 *Evaluation of Impacts of the Climatic Variable Changes and Human Activity on the Runoff and Sediment in the Yanhe Watershed North West Agriculture and Forestry University*. Northwest Agriculture & Forestry University, Xi'an.
- Schilling, K. E., Chan, K. S., Liu, H. & Zhang, Y. K. 2010 Quantifying the effect of land use land cover change on increasing discharge in the Upper Mississippi River. *J. Hydrol.* **387**, 343–345.

- Shi, H. & Shao, M. G. 2000 Soil and water loss from the Loess Plateau in China. *J. Arid Environ.* **45**, 9–20.
- Singh, H. V., Kalin, L., Morrison, A., Srivastava, P., Lockaby, G. & Pan, S. 2015 Post-validation of SWAT model in a coastal watershed for predicting land use/cover change impacts. *Hydrol. Res.* **46** (6), 837–853.
- Soil Conservation Service 1972 *Hydrology in National Engineering Handbook, Section 4*. SCS. Natural Resources Conservation Service, USA.
- Su, C. H., Fu, B. J., Lu, Y. H., Lu, N., Zeng, Y., He, A. N. & Lamparski, H. 2011 Land use change and anthropogenic driving forces: a case study in Yanhe River Basin. *Chin. Geog. Sci.* **21**, 587–599.
- Su, C. H., Fu, B. J., He, C. S. & Lu, Y. H. 2012 Variation of ecosystem services and human activities: a case study in the Yanhe Watershed of China. *Acta Oecol.* **44**, 46–57.
- Sun, Q. H., Miao, C. Y., Duan, Q. Y. & Wang, Y. F. 2015 Temperature and precipitation changes over the Loess Plateau between 1961 and 2011, based on high-density gauge observations. *Global Planet. Change* **132**, 1–10.
- Tripathi, M. P., Panda, R. K. & Raghuvanshi, N. S. 2005 Development of effective management plan for critical subwatersheds using SWAT model. *Hydrol. Process.* **19**, 809–826.
- Vasiljevic, D. A., Markovic, S. B., Hose, T. A., Ding, Z. L., Guo, Z. T., Liu, X. M., Smalley, I., Lukic, T. & Vujicic, M. D. 2014 Loess-palaeosol sequences in China and Europe: common values and geoconservation issues. *Catena* **117**, 108–118.
- Wang, D., Fu, B. J., Lu, K. S., Xiao, L. X., Zhang, Y. X. & Feng, X. M. 2010 Multifractal analysis of land use pattern in space and time: a case study in the Loess Plateau of China. *Ecol. Complex.* **7**, 487–493.
- Wei, W., Chen, L. D., Fu, B. J., Huang, Z. L., Wu, D. P. & Gui, L. D. 2007 The effect of land uses and rainfall regimes on runoff and soil erosion in the semi-arid loess hilly area, China. *J. Hydrol.* **335**, 247–258.
- Weiskel, P. K., Vogel, R. M., Steeves, P. A., Zarriello, P. J., DeSimone, L. A. & Ries, K. G. 2007 Water use regimes: characterizing direct human interaction with hydrologic systems. *Water Resour. Res.* **43**, W04402.
- Williams, J. R. & Berndt, H. D. 1977 Sediment yield prediction based on watershed hydrology. *Trans. ASAE* **20**, 1100–1104.
- Xu, J. X. 2003 Sediment flux to the sea as influenced by changing human activities and precipitation: example of the Yellow River, China. *Environ. Manage.* **31**, 328–341.
- Xu, Y. D., Fu, B. J. & He, C. S. 2013 Assessing the hydrological effect of the check dams in the Loess Plateau, China, by model simulations. *Hydrol. Earth Syst. Sci.* **17** (6), 2185–2193.
- Yan, R. H., Huang, J. C., Wang, Y., Gao, J. F. & Qi, L. Y. 2016 Modeling the combined impact of future climate and land use changes on streamflow of Xinjiang Basin, China. *Hydrol. Res.* **47** (2), 356–372.
- Yang, D. W., Shao, W. W., Yeh, P. J. F., Yang, H. B., Kanae, S. & Oki, T. 2009 Impact of vegetation coverage on regional water balance in the nonhumid regions of China. *Water Resour. Res.* **45**, W00A14.
- Zhan, C. S., Niu, C. W., Song, X. M. & Xu, C. Y. 2013 The impacts of climate variability and human activities on streamflow in Bai River basin, northern China. *Hydrol. Res.* **44** (5), 875–885.
- Zhang, X. M., Cao, W. H., Guo, Q. C. & Wu, S. H. 2010 Effects of landuse change on surface runoff and sediment yield at different watershed scales on the Loess Plateau. *Int. J. Sediment Res.* **25**, 283–293.
- Zhang, C. Q., Zhang, B. A., Li, W. H. & Liu, M. C. 2014 Response of streamflow to climate change and human activity in Xitiaoqi river basin in China. *Hydrol. Process.* **28**, 43–50.
- Zhu, Y., Wang, W., Liu, Y. & Wang, H. J. 2015 Runoff changes and their potential links with climate variability and anthropogenic activities: a case study in the upper Huaihe River Basin, China. *Hydrol. Res.* **46** (6), 1019–1036.

First received 14 June 2016; accepted in revised form 5 November 2016. Available online 6 January 2017